On the Thermal Evolution of Passive Continental Margins, Thermal Depth Anomalies, and the Norwegian-Greenland Sea

GARY W. ZIELINSKI[1]

Department of Geological Sciences and Lamont-Doherty Geological Observatory
Columbia University, Palisades, New York 10964

A computer model of sea floor spreading is presented. This time-dependent thermal model, which includes the presence of an adjacent continent, simulates not only the evolution of an oceanic region but also the thermal evolution of an Atlantic-type continental margin. Incorporation of the adjacent continent into a sea floor spreading model allows one to utilize geological and geophysical data from the continent and continental margin as constraints. In terms of the model parameters a more complete picture of the early spreading history and its relation to the initial rifting of the continent is provided. While vertical heat flow dominates in both the ocean and the continent proper, several effects of lateral heat flow across the ocean-continent boundary are seen. They are reflected in the surface heat flow and topography computed from the model. Owing to lateral heat flow, subsidence of the continental margin can be more rapid than has been estimated from previous models and is a strong function of horizontal position. Applied to the Norwegian-Greenland Sea, the model satisfies all available geophysical data for that area and produces oceanic depths nearly 1 km shallower than for other oceans of comparable age. It is consistent with the idea that thermal expansion is responsible for the unusually shallow depths and positive free air gravity observed in the Norwegian-Greenland Sea. These results may be applicable to parts of other oceans where large regions depart from the normal age-depth curve. Thermal depth anomalies are not necessarily indicative of increased heat input from below but may more generally reflect differences in the ratio of the heat entering the lithosphere to the spreading rate. If it is correct, this concept may provide an origin for some of the shorter-wavelength relief (10–100 km) seen in oceanic basement. The heat flow distribution across the Norwegian continental margin is consistent with a thermal model in which the Vøring Plateau Escarpment is concident with the ocean-continent boundary.

INTRODUCTION

One method for investigating the implication of a surface heat flow distribution on processes occurring at depth in the earth is through the use of thermal models [e.g., *Langseth et al.*, 1966; *McKenzie*, 1967]. In these models the oceanic lithosphere is assumed to behave as a moving two-dimensional slab of material which cools conductively through its upper surface as it moves away from a vertical boundary held at the melting temperature. Although such models are likely to be gross oversimplifications of what occurs in nature, they serve to group causes into a finite number of categories. For this reason they can provide a unified set of parameters for comparing one region with another. With this in mind a thermal model has been developed in order to compare the Norwegian-Greenland Sea, as represented by the Mohns Ridge spreading center, with other world ocean spreading centers.

The Mohns Ridge spreading center (Figure 1) provides a unique opportunity to constrain sea floor spreading models. Not only are there reliable heat flow measurements distributed uniformly over the age range of that spreading center [*Langseth and Zielinski*, 1974], but also there are a series of reliable heat flow measurements on the Norwegian continental margin, and from *Swanberg et al.* [1973], borehole measurements of heat flow and radioactive heat generation on the adjacent continent in Norway. Thus a two-dimensional model encompassing the Mohns Ridge spreading center, the continental margin, and the adjacent continent would be constrained by surface heat flow measurements along its entirety.

THE MODEL

The model envisioned is one in which at time zero the continent is intruded by new oceanic material at the melting temperature and begins to move laterally at some fixed spreading rate. As the motion continues, newly formed ocean fills the void left by the moving continent, and the development of the area can be followed through time. The equation and boundary conditions solved are

$$\frac{1}{\mathbf{K}}\left\{\frac{\partial T}{\partial t}+v\frac{\partial T}{\partial x}\right\}=\frac{\partial^2 T}{\partial x^2}+\frac{\partial^2 T}{\partial z^2}+\frac{Q}{K}$$

$T = 0$ $(z = 0)$, $T = 1{,}330°\text{C} + 0.6°\text{C/km}$ $(x = 0)$ [*Jordan*, 1975], $K(\partial T/\partial z) = F_B$ $(z = L)$, $\partial T/\partial x = 0$ $(x = 2{,}000$ km), where T is temperature, t is time, $\mathbf{K}$ is the thermal diffusivity, K is the thermal conductivity, V is the spreading rate, Q is heat generation, and x and z are taken in the horizontal and vertical directions, respectively. Tm is the melting temperature, F_B is the heat flow through the bottom boundary, and L is the verticle thickness of the region. The bottom boundary should be placed at a depth where differences in thermal properties between ocean and continent are sufficiently small that vertical heat flow may be assumed. *Froidevaux et al.* [1977] argue that the temperature beneath old oceans and stable continents should become equal somewhere between 200- and 400-km depth. Since according to *Clark and Ringwood* [1964], heat generation should also be equal in that range, the bottom boundary will initially be placed at 400 km. Some consequences of smaller values of L will be discussed.

Because of the large time constant for thermal processes within the earth, heat flow data from the oceans cannot constrain the heat flux at 400 km. This can, however, be derived from the continental geotherm if steady state one-dimensional heat flow is assumed.

[1] Now at Geological Sciences Department, Gulf Science & Technology Company, Pittsburgh, Pennsylvania 15230.

Paper number 9B1004.
0148-0227/79/009B-1004$01.00

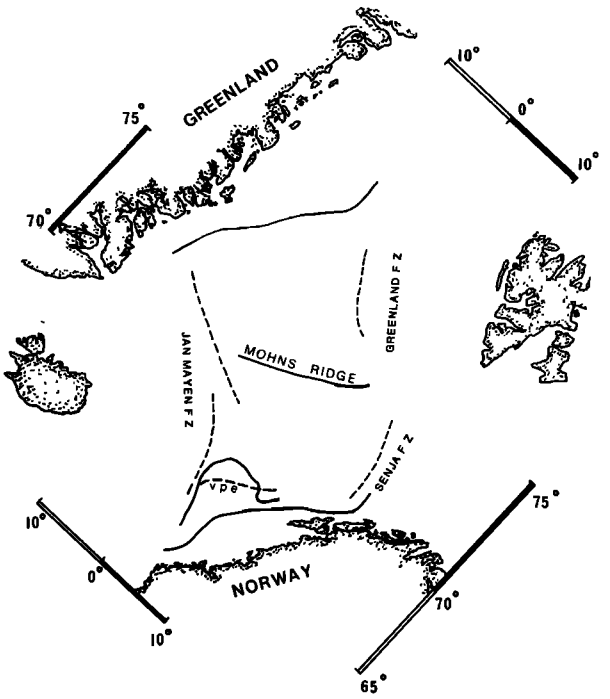

Fig. 1. Sketch map showing the location of the Mohns Ridge spreading center in relation to adjacent land masses, bounding fracture zones, and the Vøring Plateau Escarpment (vpe) [after *Talwani and Eldholm,* 1977].

Swanberge et al. [1973] have reported heat flow and heat generation measurements from four geologic provinces in Norway. On the basis of their data, a heat flow value of 48.1 mW/m^2 (1.15 HFU, 1 HFU = 1 μcal/cm^2 s) seems reasonable for continental Norway adjacent to the Vøring Plateau. If an exponentially decreasing heat source distribution with depth is assumed [*Lachenbruch,* 1970], a surface heat generation of about 3.3×10^{-6} W/m^3 (8 HGU, 1 HGU = 10^{-3} cal/cm^{-3} s^{-1}) with a logarithmic decrement of 8.4 km can be deduced from *Swanberg et al.* [1973]. Beneath the logarithmic layer, a constant heat generation of 4.6×10^{-8} W/m^3 (0.11 HGU) is assumed. This value corresponds to the heat generation for pyrolite II [*Sclater and Francheteau,* 1970] and produces a deep geotherm similar to that of *Minister and Archambeau* [1970] and *Froidevaux and Schubert* [1975].

With boundary conditions of zero surface temperature and a heat flow of 48.1 mW/m^2 (1.15 HFU), the steady state heat flux at depth can be solved for. At 400 km the models predict a heat flux of only about 1.7 mW/m^3 (0.04 HFU). This heat flux is assumed for the bottom boundary, F_B.

COMPUTATIONAL SCHEME

The model described in the previous section forms an initial value problem which can be solved by standard finite difference techniques [e.g., *Langseth et al.,* 1966; *Bottinga and Allegre,* 1973]. The initial temperature distribution (Figure 2*a*) is provided by the continental geotherm computed for Norway. At time zero, the ocean-continent boundary, coincident with the ridge axis boundary, begins to move with the entire slab at a spreading velocity V of 1 cm/yr [*Talwani and Eldholm,* 1977]. At subsequent times, on and to the right of the ocean-continent boundary, the 'continental' heat source distribution is maintained. To the left of the boundary, an 'oceanic' heat source distribution is maintained which is also assumed to be exponential with depth, however, with a surface heat generation of 5.0×10^{-7} W/m^3 (1.2 HGU) and logarithmic decrement of 25 km. As in the case of the continental distribution, a value of 4.6×10^{-8} W/m^3 (0.11 HGU) is assumed below the logarithmic layer. The resulting distribution is a good approximation to the geochemical model of *Clark and Ringwood* [1964] and meets the condition of constant thermal properties at 400 km.

In all of the computations the horizontal grid spacing was given a value of 10 km in regions such as near the ridge axis or the ocean-continent boundary, where large temperature gradients were anticipated or high resolution was desired. Elsewhere, it was increased to 50 km. In the vertical direction the grid spacing was increased in an arithmetic progression from 3 km at the surface to 48 km near 400 km. The time step was of the order of 65,000 years (for more details, see *Zielinski* [1977]). Thermal diffusivity is taken to be a constant 0.009 cm^2/s [*Zielinski,* 1977]. Partial melting at the base of the lithosphere was considered, however, for values less than 10%; effects were found to be negligible. Sample temperature output at 0, 10, 30, and 60 m.y. is shown in Figure 3, with oceanic regions shaded.

Heat flow was computed by fitting a second-order polynomial to the temperatures at the upper three nodes, computing the gradient at the surface, and multiplying by a surface thermal conductivity of 2.9 W/m°C (7 mcal/°C cm s) [*Schatz and Simmons,* 1972].

If density is assumed to be a function of temperature, the resulting surface topography can also be computed from the temperature field [*Langseth et al.,* 1966; *Sclater and Francheteau,* 1970]. In doing such computations, most workers have used the steady state ocean as a reference from which changes in topography were computed. For the model being presented, it has been more convenient to use as a reference an ocean at zero temperature throughout. Doing so allows one to compare topographic profiles of several models with differing thermal regimes to a common density reference.

Two mechanisms for isostatic adjustment are considered here. The first is the compensation by asthenospheric material for the sea water displaced by expansion and contraction of the oceanic lithosphere. This mechanism occurs on the oceanward side of the continental margin. In the second mechanism the density of the continent is chosen so that for a steady state temperature distribution its surface is at sea level and is in isostatic equilibrium with respect to the adjacent ocean. The second adjustment mechanism therefore gives rise to a difference in elevation due to the density contrast between ocean and continent. The oceanic block and the continental block are assumed to be completely decoupled with constant pressure at a depth of 400 km.

The constants assumed for the topographic calculations presented are as follows: the zero temperature ocean density and the density of the asthenosphere are both taken to be 3.33 g/cm^3. To produce realistic ocean depths, the zero-temperature continent must have a density of about 2.83 g/cm^3. The density of sea water is 1.03 g/cm^3, and the thermal expansion coefficient is assumed to be 3.22×10^{-5} °C^{-1} [*Forsyth,* 1977].

The initial continental temperature distribution for most of the models presented is shown in Figure 2*a*. The left-hand boundary of the slab is at the melting temperature. Plotted above the slab is the topographic uplift due to thermal expansion. For the usual initial conditions, the uplift is in the form of a spike over the melting temperature boundary. This uplift rapidly broadens in time, however, initially it is unrealistic. A

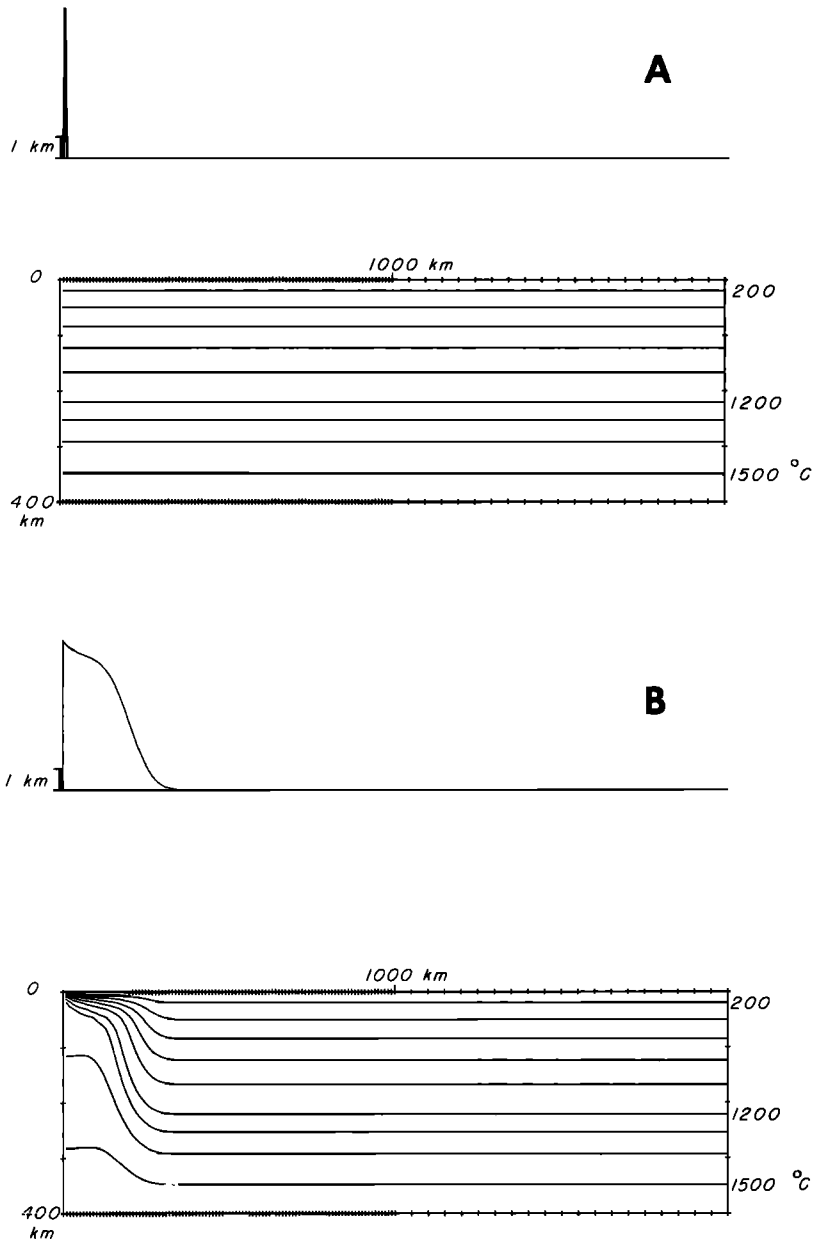

Fig. 2. The isotherms for two continental slabs at the onset of sea floor spreading (left-hand edges at the melting temperature). Above each slab is shown the topographic uplift due to thermal expansion with respect to a steady state continent. A thermal expansion coefficient of 3.22×10^{-5} °C^{-1} is assumed. Figure 2*a* represents the initial conditions assumed for most of the modeling. Figure 2*b* represents a continent which has remained stationary for a period of 20 m.y. prior to the onset of sea floor spreading. During that period, the continent has undergone heating by lateral conduction and convection from the left-hand edge.

somewhat more realistic approximation is explored in Figure 2*b*, where the onset of sea floor spreading is delayed by 20 m.y. During this period of time, the stationary continent undergoes heating by conduction and convection associated with the intrusion of magma from the axial zone. Such a situation might be analogous to a period of continental rifting prior to sea floor spreading. Isotherms show a shallowing, and a much broader area is already uplifted by the time spreading commences. Some results of this case will be seen later.

TEMPERATURE RESULTS

Figure 4 shows the temperature fields for two models at 160 m.y. for comparison with oceans older than the Norwegian-Greenland Sea (MR denotes Mohns Ridge; WO denotes world oceans). The vertical solid line within the slab shows the position of the ocean-continent boundary. For the WO model, maximum temperatures at 400 km are a little more than 1,600°C, and for MR, temperatures are less than 1,700°C at 400 km. Each of these models therefore yields temperatures at 400-km depth, which is not excessively high even beneath the oceans. The two models differ only in the temperature gradients assumed at the ridge axes, MR being greater than WO by 0.2°C/km.

The most dramatic effect of the presence of oceanic heat generation is a warming of the oceanic material with age below about 200-km depth, as seen in the rise of the deeper isotherms with age. This may, in part, be accentuated by the particular choice of the temperature boundary condition at the

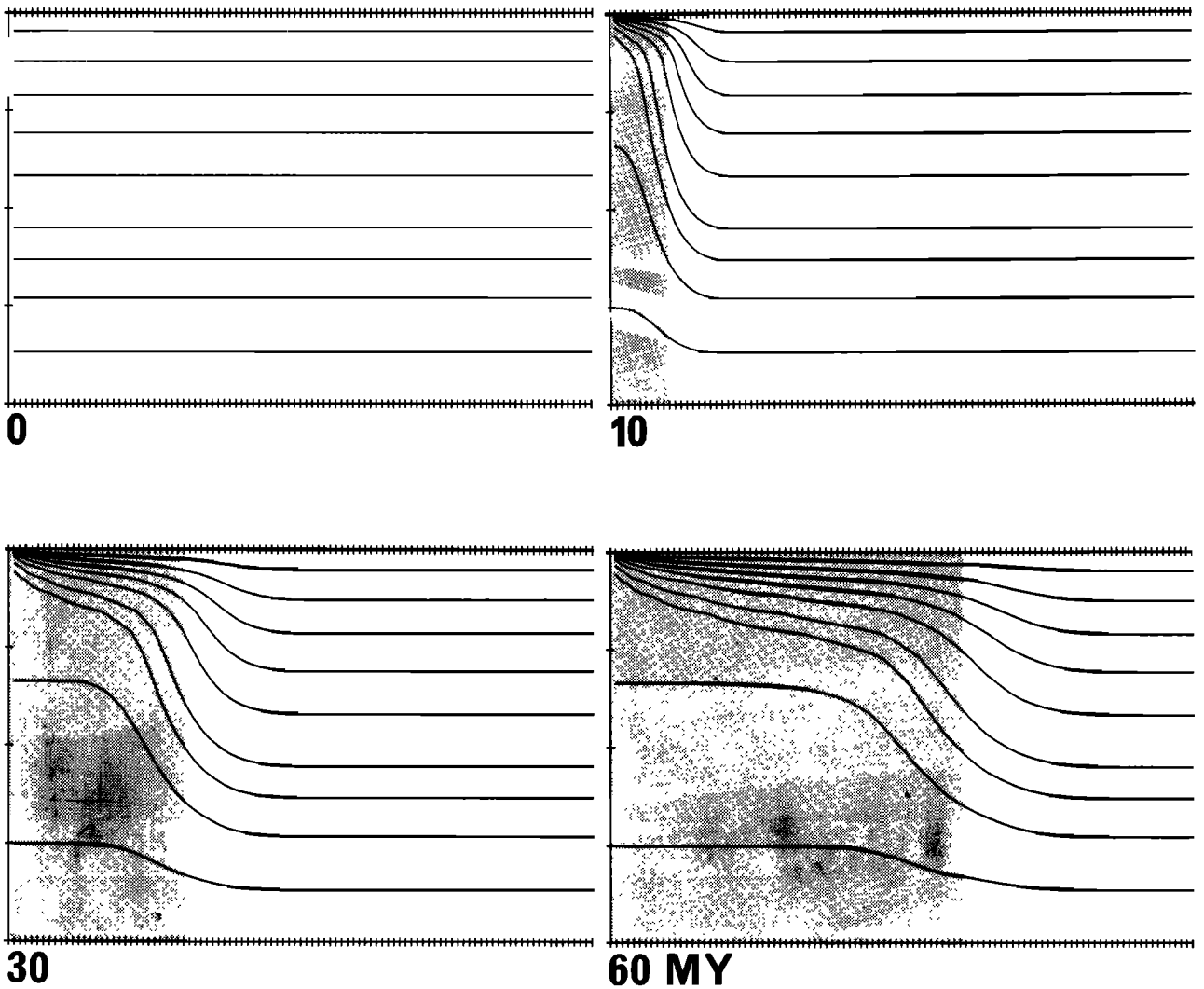

Fig. 3. Sample temperature output from the computer model of 0, 10, 30, and 60 m.y. The darkened region is newly formed 'ocean.' (Dimensions and isotherms are the same as they are for Figures 3 and 5.)

ridge axis. The effect, however, completely disappears when the oceanic heat generation is removed.

Intermediate temperatures are also affected by the heat source distribution. The position of the base of the oceanic lithosphere from a compilation of seismic surface wave data [*Forsyth*, 1977] is shown by the solid circles plotted in each of the slabs in Figure 4. It is in reasonable agreement with the rough position of the solidus of possible lithospheric materials (e.g., periodotite, less than 0.4% water), the stippled region. The presence of sufficient heat generation in the oceans maintains the temperature field in good agreement with the surface wave data. Without oceanic heat sources, more heat flux from below would be required to prevent the thickness of the oceanic lithosphere from becoming too great.

The general features of the temperature fields produced by these models are as follows: the temperature field in the upper 100 km reflects the thermal boundary layer corresponding to the formation of oceanic lithosphere. Below the boundary layer depth, the relative flatness of the 1,400°C and 1,500°C isotherms as followed away from the ridge indicate that no heat is being conducted laterally from the ridge axis. To this approximation, for $V = 1$ cm/yr the fact that the lower 200 km of the region is also in lateral motion (i.e., not just the lithosphere) is of little consequence thermally. Below 200 km, the temperature beneath the ridge could be brought into better agreement with the continental geotherm by choosing smaller values of *Tm* down to about 1,200°C and adjusting other parameters accordingly. Still, the temperatures produced here are within the range for acceptable rheologies [*Froidevaux et al.*, 1977].

Within about 300 or 400 km of the ocean-continent boundary, a marked deepening of the oceanic isotherms is seen. This effect, corresponding to the transition from the younger relatively warm oceanic region to the colder continent, continues an equal distance onto the continent until steady state heat flow is attained. In these models the magnitude and wavelength of the temperature transition is largely a function of the age difference between the ocean and continent (see Figures 3 and 4). The contrast in heat production also affects the transition but to a lesser degree.

HEAT FLOW AND TOPOGRAPHY

The two strongest constraints imposed on the model by geophysical data are the observed surface heat flow and the topography. They differ from each other in that the large time constant associated with surface heat flow is absent in topography. Both, however, reflect the subsurface temperature field.

Figure 5 summarizes the heat flow data associated with the

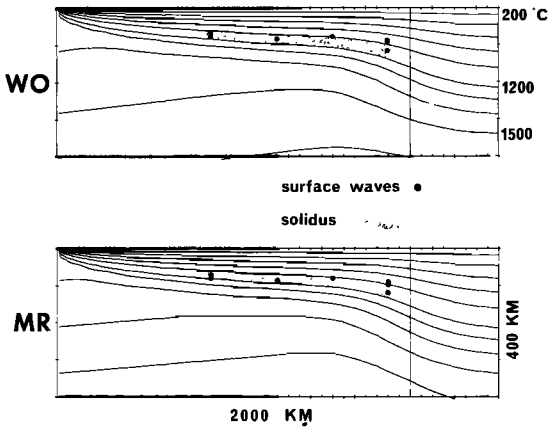

Fig. 4. Temperature fields at 160 m.y. for two thermal model outputs. (MR denotes Mohns Ridge; WO denotes world oceans). The left edges represent ridge axes at the melting temperature. The vertical line through each slab marks the position of the ocean-continent boundary. The solid circles mark the base of the oceanic lithosphere from seismic surface wave data compiled by *Forsyth* [1977], and the stippled region is the same approximate parameter based on the wet solidus of peridotite (<0.4% water).

Mohns Ridge spreading center. While the Mohns Ridge heat flow data, in general, fall above the *Sclater and Francheteau* [1970] North Pacific data, when viewed in comparison with the reliable North Pacific heat flow from *Sclater et al.* [1976], the Mohns Ridge heat flow does not appear anomalously high. The significant departure of the *Sclater and Francheteau* [1970] data from the 'reliable' North Pacific data can be explained if heat loss from hydrothermal circulation is present in the former data set. The latter data set has been screened to include only stations where hydrothermal circulation is not likely to be occurring. Where the Sclater and Francheteau data can be shown to depart from theoretical heat flow, predicted by slab models, the reliable data seem to be in fairly good agreement. Therefore it is possible that the Mohns Ridge heat flow is simply a better indicator of theoretical heat flow than other oceans. This could in turn imply that hydrothermal circulation, considered likely to be taking place in many of the world oceans, is not as prevalent in the Norwegian-Greenland Sea. This conclusion is supported by the fact that none of the axial low heat flow values often associated with hydrothermal circulation have been reported for the Norwegian-Greenland Sea [*Langseth and Zielinski,* 1974]. Shown also in Figure 5 is the theoretical heat flow curve calculated from models MR and WO. (Both models produce the same theoretical heat flow.) Since the data do not imply a significant heat flow difference between the Mohns Ridge and the other world oceans, a single curve is sufficient to fit both data sets.

Figure 6 is a compilation of topographic data. The detailed drawing of the crestal region of the Mohns Ridge is from *Johnson* [1974]. On the age-depth plot the solid circles represent 19 data points picked off seismic profiles across the Mohns Ridge at well-identified magnetic anomalies [from *Talwani and Eldholm,* 1977] and corrected for isostatic sediment loading. The comparable data for the world oceans [*Parsons and Sclater,* 1977] fall within the envelope formed by the dot-dash curves. The relative subsidence of the Mohns Ridge, based on the data points, seems to be no different from the subsidence of the rest of the world ocean ridges; however, basement depths for the Mohns Ridge are uniformly shallower by nearly 1 km. It has been demonstrated that the gross ocean floor topography can be explained as being thermal in origin [*Sclater et al.,* 1971]. It may therefore be reasonable to seek an explanation for the depth anomaly in the Norwegian-Greenland Sea in terms of a temperature anomaly in the upper several hundred kilometers. If the shallow sea floor in the Norwegian-Greenland Sea is in fact related to thermal expansion, it may be indicative of a regional 'hot spot' not evident in the heat flow data. Conversely, any thermal mechanism which successfully duplicates the topographic anomaly must do so without giving rise to an obvious heat flow anomaly. One such mechanism may be reflected in model MR, which provides a good fit of the Mohns Ridge age-depth data (Figure 6) as well as the heat flow data in Figure 5.

The change in thermal regime, shown by the models near the continental margin, is also reflected in the surface heat flow. Two effects predicted by the thermal model presented here are illustrated in Figure 7. Isotherms computed by the model are shown at age 60 m.y. for slabs 100 km thick (the isotherms extend only to 60 km). Above each slab is plotted the theoretical heat flow through its surface. Figure 7*a* illustrates an edge effect in the heat flow which will be called the 'long-wavelength' edge effect. This effect is the result of the general deepening of the isotherms as the transition is made from ocean to the much older continent. In the model used to illustrate this effect, there was no difference between ocean and continent heat production. When a difference is assumed, as it is in most of the cases presented here, another form of edge effect arises in the heat flow. Comparing the continent and ocean heat productions discussed earlier, there can be seen a very large discontinuity in crustal heat sources at the ocean-continent interface. Because of this discontinuity, there is a very shallow component of heat flow from the continent into the ocean, which attempts to balance the offset in heat production. Only the upper 25 km or so are involved in the process, so that this edge effect can be considered near surface or 'short wavelength' compared with the previous. An example of the combined long- and short-wavelength edge effects is shown in the temperature field and associated heat flow in Figure 7*b*. It is of interest to consider these edge effects

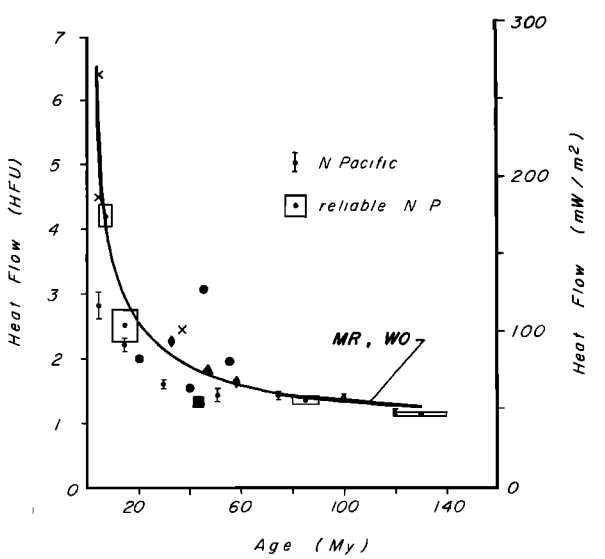

Fig. 5. Mohns Ridge heat flow versus age. The curve is theoretical heat flow for the Mohns Ridge (MR) and world oceans (WO) models. Also shown are the North Pacific data from *Sclater and Francheteau* [1970] and the reliable North Pacific data from *Sclater et al.* [1976].

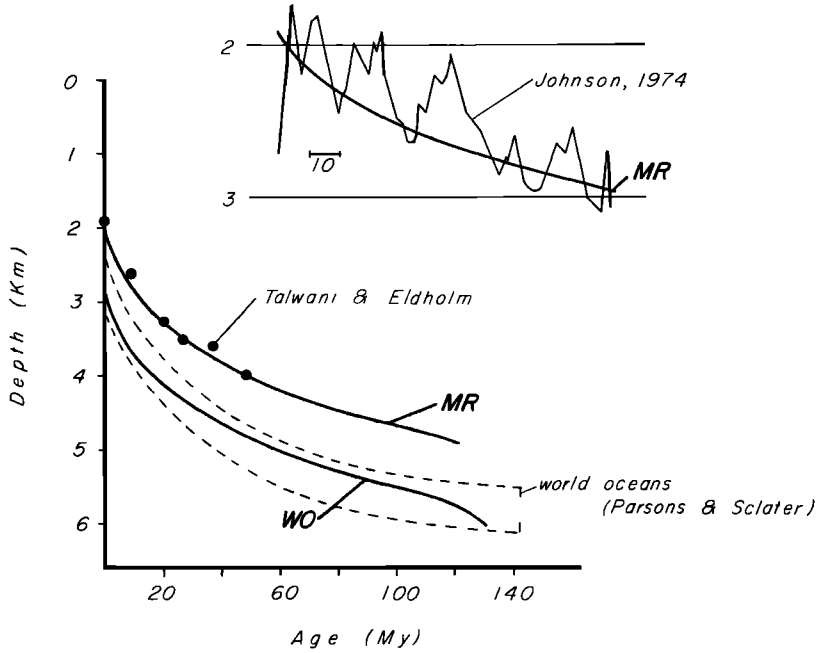

Fig. 6. Mohns Ridge depth versus age. Solid circles are from *Talwani and Eldholm* [1977] and the inset profile from *Johnson* [1974]. The solid curves are computed from thermal models for the Mohns Ridge (MR) and world oceans (WO). The dash-dot lines represent the range of age-depth data for the world oceans [*Parsons and Sclater*, 1977].

in examining the distribution of heat flow across the Vøring Plateau Escarpment.

Heat Flow Across the Continental Margin

The Vøring Plateau Escarpment has been interpreted by *Talwani and Eldholm* [1972] as marking the site of an Early Tertiary opening of the Norwegian-Greenland Sea. According to their interpretation, seaward of the escarpments, normal oceanic crust began to form via the sea floor spreading mechanism and has continued to do so to the present. Landward of the escarpments, one should expect to find basement which is essentially continental.

The reliable heat flow stations have been plotted relative to the Vøring Plateau Escarpment (Figure 8, the open symbols). The circles are from *Haenel* [1974], and the triangles are from *Zielinski* [1977]. The solid symbols represent the heat flow corrected for topography and sediment refraction. Also shown landward of the escarpment is the mean regional heat flow (the horizontal line) estimated from the measurements. The dominant feature of the data, the marked decrease in heat flow as the Vøring Plateau Escarpment is approached from seaward, cannot be significantly reduced by environmental correction. For comparison, the solid line marked 'no continent' shows the slope the heat flow would have due to simple ocean cooling in the absence of an adjacent continent. The theoretical heat flow from the models in Figure 5 has been continued onto the continental margin in Figure 8, assuming that the theoretical ocean-continent boundary is coincident with the Vøring Plateau Escarpment. The dashed curve is for a model with no oceanic heat sources. In Figure 8 the decrease in heat flow from the ocean to the escarpment predicted by the models is significantly greater than the 'no continent' decrease, providing a much better fit to the data in that region. Since it is unlikely that the heat flow distribution is caused by the local environment, some deeper cause must be sought. One interpretation is that it is an expression of a heat flow edge effect due to the ocean-continent boundary being coincident with the Vøring Plateau Escarpment.

Continental Margin Evolution

Model MR has been shown to be in good agreement with all theoretical and data-related constraints for an ocean formed via sea floor spreading and bounded by an old (Precambrian to Early Paleozoic) continent. In addition, it produces ocean floor topography nearly a kilometer shallower than for other world oceans. For these reasons it may be considered representative of the Norwegian-Greenland Sea and, in particular, the Mohns Ridge spreading center. Figure 9 shows the topographic output from MR at 10, 30, and 60 m.y., showing the theoretical thermal evolution of the Norwegian-Greenland Sea to present time. In Figure 9 the evolution is allowed to continue 100 m.y. beyond present to 160 m.y. From left to right, the early portion of the topographic curve shows the normal ocean ridge subsidence. The more rapid deepening at the continental margin is analogous to the heat flow edge effect (Figure 7*a*) and is also due to the deepening of isotherms as the continent is approached.

As the sea floor adjacent to the continent deepens with age, the edge effect broadens and becomes less pronounced. To the right of the ocean-continent boundary, the uplifted continent (shaded) is also seen to undergo a change in time. The amplitude of the uplift diminishes due to cooling; however, the uplifted area becomes broader as heat is diffused laterally into the interior of the continent.

Several processes such as erosion, deposition, and sediment loading have been ignored in these models. Those parts of the continental margin which are thermally uplifted above sea level would be expected to simultaneously undergo considerable erosion [*Foucher and Le Pichon*, 1972]. As a result of the removal of the eroded material, isostatic rebound would then result in further uplift. Subsequent deposition of the eroded material onto the adjacent oceanic area also plays an important part in shaping the continental slope. None of the features are included in the models presented here. In this respect, the model topography represents a fundamental profile governed primarily by a response to temperature. Never-

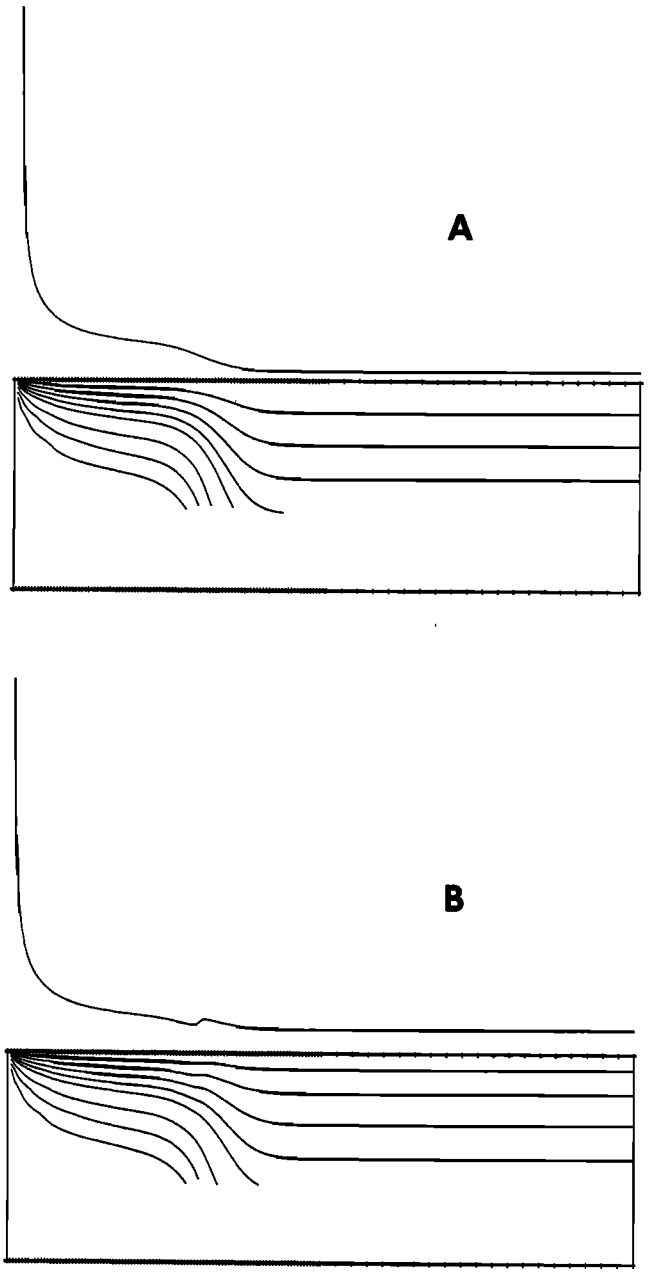

Fig. 7. Temperature fields with heat flows plotted above for two 100-km-thick slab models at 60 m.y., illustrating the effects on the temperature field of transition from ocean ridge to continent (left to right). Figure 7*a* shows an exaggerated drop in heat flow across the ocean-continent boundary with no discontinuity in heat generation (the long-wavelength effect). Figure 7*b* combines the above effect (unexaggerated) with a shorter-wavelength effect due to the discontinuity in heat generation (ocean to continent) assumed for the models presented (the short-wavelength effect).

theless, several features of the model may be directly relatable to actual continental margins. *Walcott* [1972] has shown that it is difficult to account for thick sediments found on some narrow margins by loading alone. This leaves open the possibility that some control might be exercised by the temperature field, i. e., a deepening of oceanic basement beneath continental margins may be an expression of a thermal edge effect. The topographic discontinuity between ocean and continent in the models represents a region of decoupling between the two. Geologically, this could be pictured as a zone of marginal faulting.

Earlier, it was mentioned that a model was tested in which the continent was allowed to heat up during a period of rifting 20 m.y. prior to the onset of sea floor spreading. The resulting topography at 60 m.y. for this case is shown in Figure 9, the dashed curve. Note the absence of the edge effect at the continental margin, apparently offset by the higher initial temperatures in the trailing edge of the continent. Over the continent, the remnant of greater initial uplift is still quite strong at 60 m.y.

Holtedahl [1960] published a map of Cenozoic uplift, believed to be of tectonic origin, across Scandanavia. In Figure 10 the Holtedahl data along section AA′ is plotted on a graph of uplift versus distance. The zero point on the horizontal axis is the Norwegian shoreline, and the vertical axis coincides with the position of the Vøring Plateau Escarpment. The continental uplift from Figure 9 at 60 m.y. is plotted along with the Holtedahl data. The solid curve is for the simple initial condition (Figure 2*a*), and the dashed curve *a* for the 'rifting' initial condition (Figure 2*b*). Note that the solid curve is considerably more displaced from the data than dashed curve *a*. This implies that with the simple initial condition an insufficient portion of the continent is affected thermally. The better fit of dashed curve *a* can be improved if it is assumed that all material uplifted above sea level is rapidly eroded, and more uplift is allowed via isostatic rebound (dashed curve *b*).

In light of the crude vertical temperature boundary condition used for the ridge axis, there is reasonably good agreement between the slope of the theoretical uplift curves and the data. Use of an axial boundary condition as in the work of *Langseth et al.* [1966] and *Bottinga and Allegre* [1973] which distributes the ridge axis melting temperature over a sloping (not vertical) surface would probably cause the theoretical uplift to be less steep than in Figure 10 and provide a better fit to the data.

It may also be seen in Figure 10 that theoretical maximum uplift of the continent edge can be of the order of 5 km or more. Widespread Tertiary uplift is reported for East Greenland [*Haller,* 1971] with amounts of up to 8 km inferred for some areas [*Wager,* 1947] (some of this may postrifting). Reference made to the Miocene-to-recent Baikal arch and rift system with uplifts of 5–7 km further seems to agree in magnitude with the uplift predicted by the theoretical models. Despite these examples there are areas like the North Sea where the geologic data show no evidence for large-scale uplift associated with a rifting thermal event. Such areas have prompted alternate mechanisms, such as lithospheric stretching [*McKenzie,* 1978], to explain the observed postrifting subsidence. The need for these alternate mechanisms on most Atlantic-type continental margins and rift zones, however, is a point still in question, awaiting further synthesis of the data in these areas.

While the computed ocean floor topography rapidly assumes steady state from point to point (i.e., the ocean depth 300 km from the ridge axis is the same at 160 m.y. as it is at 60 m.y.), the same is not true for points on the continental margin. In this region the model may be used to compute subsidence rates. Some results are shown in Figure 11, a plot of thermal subsidence of the edge of the continent as a function of age. The subsidence curves in Figure 11 also ignore the effects of erosion and sediment deposition. They are in a form, however, which can be directly compared with recently published data based on deep wells and seismic lines that have been 'backstripped' [Watts and *Ryan,* 1976]. Curve *a* is for a 400-km slab and curves *b*, *c*, and *d* are for a 60-km slab. In the

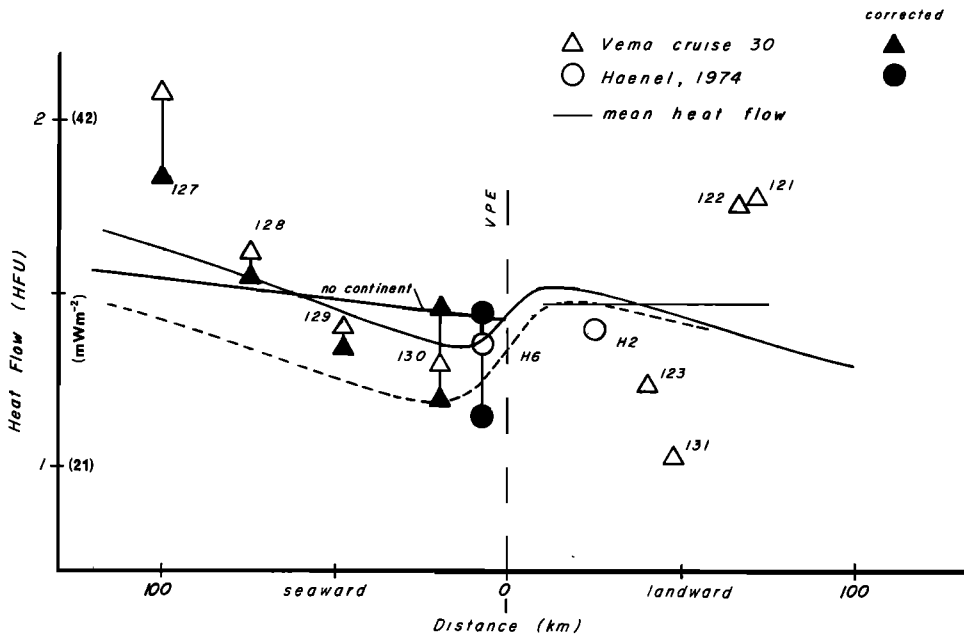

Fig. 8. Heat flow data (open symbols) on the Vøring Plateau plotted with respect to the Vøring Plateau Escarpment (vertical dashed line). Solid symbols are corrected for maximum topography and sediment refraction effects. The circles are heat flow measurements from *Haenel* [1974]. The horizontal line landward of the Vøring Plateau Escarpment indicates the mean regional heat flow from the data. The solid line (seaward) marked 'no continent' shows the horizontal change in heat flow a model would have in the absence of the continent. Theoretical heat flows for Mohns Ridge and world oceans (solid curve) and for an ocean with no heat generation from radioactive sources (dashed curve) are shown.

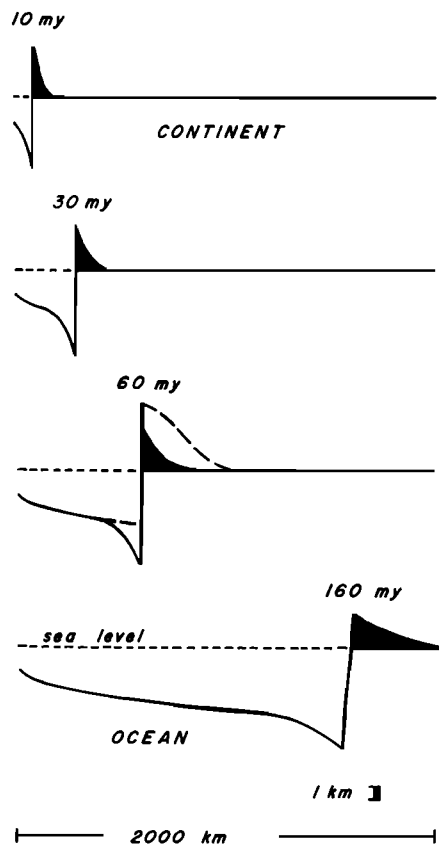

Fig. 9. Topography computed from the thermal model MR at 10, 30, 60, and 160 m.y. The shaded regions are the portions of the continent thermally uplifted above sea level. The dashed curve at 60 m.y. is for the 'rifting' initial condition (Figure 2*b*), whereby the continent undergoes a 20-m.y.-long period of heating prior to sea floor spreading.

first 10 m.y., curve *a* shows over 3 km of subsidence. Subsequent to that time, there is little difference between the subsidence shown by *a* and *b*.

Sleep [1971] successfully utilized a thermal model in analyzing subsidence of the Atlantic continental margin, but argued that one-dimensional models were sufficient to explain subsidence due to thermal contraction. For the purpose of comparing a one-dimensional model with the model presented here the early subisdence of a comparable cooling half space is also plotted in Figure 11 (solid circles). With respect to the half space, curve *b* appears to have lost a larger proportion of

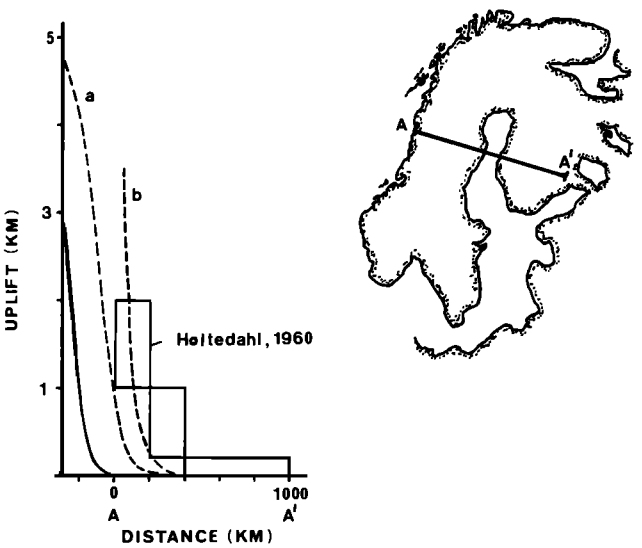

Fig. 10. Oblique uplift across Scandanavia [after *Holtedahl,* 1960] along section AA'. Plotted along with the data are theoretical curves from model MR. Curve *a* is replotted from Figure 9 (dashed), and curve *b* shows additional uplift due to erosion.

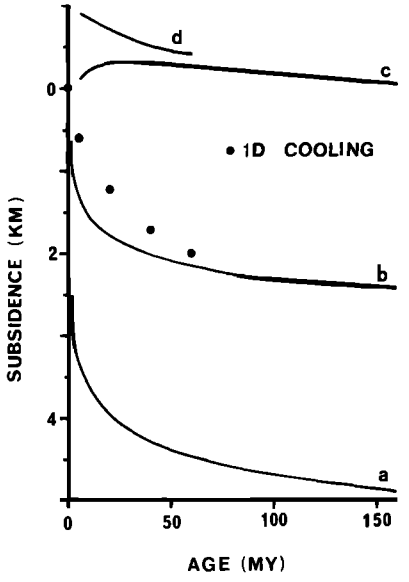

Fig. 11. Thermally induced subsidence (relative to position at time zero) of the continent edge versus age for (*a*) L = 400 km and (*b*), (*c*), and (*d*) L = 60 km for several models (solid curves). Curves *d* and *c* are for points 10 and 50 km inland. The solid circles show the first 60 m.y. of subsidence predicted by a comparable cooling half space.

heat within the first 20 m.y. This is evidenced by the greater subsidence in that interval. Subsidence data from the Gulf of Lion [*Watts and Ryan,* 1976] show more rapid initial subsidence when compared with the empirical ocean ridge subsidence curve of *Hays and Pitman* [1973].

The more rapid initial subsidence shown possible in Figure 11 can be attributed to early lateral heat loss through the ocean-continent boundary. Figure 12 is a plot of horizontal temperature gradients across the ocean-continent interface at 5, 10, 30, and 60 m.y. The dashed lines indicate heat flow, assuming a thermal conductivity of 2.9 W/m°C (7 mcal/°C cm s). At 60 m.y., it can be seen that heat loss due to conduction across the continental margin is only a fraction of the heat loss through the ocean floor (less than 4.2 mW/m^2 vertically through a 600-km-wide ocean floor). At 5 m.y., however, the corresponding amounts indicate a different situation. At that time, the heat loss through the ocean floor crestal region may be as high as 300 mW/m^2 through a 50-km-wide surface. The lateral heat flow, while only averaging about 21 mW/m^2, would yield heat loss of comparable magnitude if it occurred through a 400-km interface. The strong dependence of initial subsidence on slab thickness L (Figure 11) can be explained by the distribution of horizontal thermal gradient with depth in Figure 12. The average heat flow across the interface changes with the particular thickness assumed. This is due to the change in gradient with depth. However, by increasing or decreasing that thickness, the 'window' through which heat is transferred is also opened or closed.

The lateral heat flow indicated in Figure 12 is for models starting with the simple initial condition of the left edge of a cold continent being at the melting temperature. The more realistic rifting initial condition would cause a shift in the time axis, producing a smaller ocean-continent temperature contrast for a given interval of spreading. Figure 12, for that reason, probably illustrates maximum horizontal gradients.

Curves *a* and *b* in Figure 11 have been computed for a point exactly at the edge of the continent, and curves *d* and *c* illustrate the vertical motion for points 10 and 50 km farther onto the continent. Both latter points become uplifted sometime after the onset of sea floor spreading (best illustrated by curve *c*). It is evident from Figure 11 that one point on a margin could be undergoing thermal uplift while another point some lateral distance away is subsiding. The absolute rates of vertical motion are also seen to diminish rapidly with distance from the continent edge.

The results shown in Figure 11 are also for the simple initial condition. One effect of using the rifting initial condition would be that the decreasing subsidence with distance from the continent edge would be more gradual and probably, for that reason, more realistic.

THERMAL DEPTH ANOMALIES

Model MR and model WO differ in only one of their input parameters, the magnitude of the linear temperature gradient assumed at the ridge axis. This difference ~0.2°C/km (greater for MR) results in ocean depths nearly a kilometer shallower

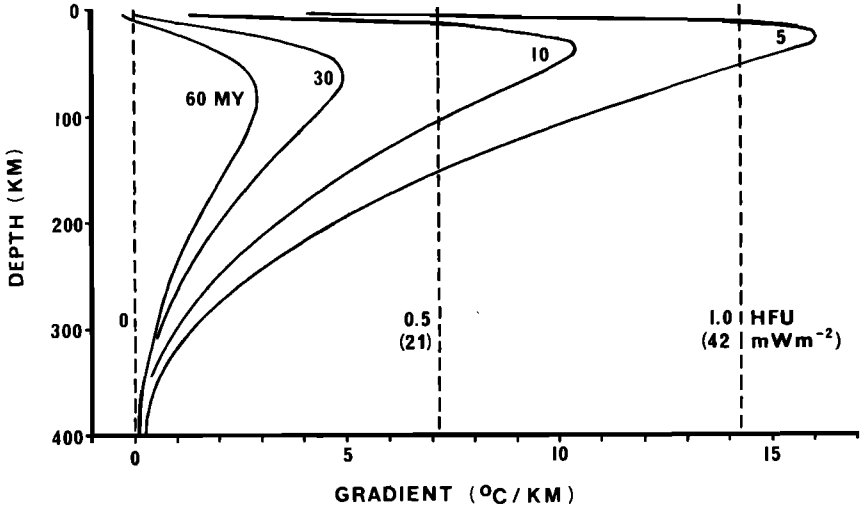

Fig. 12. Horizontal thermal gradient across the ocean-continent interface versus depth, computed from model WO at 5, 10, 30, and 60 m.y. The vertical dashed lines show corresponding heat flow for a thermal conductivity of 2.9 W/m°C (7 mcal/s °C cm).

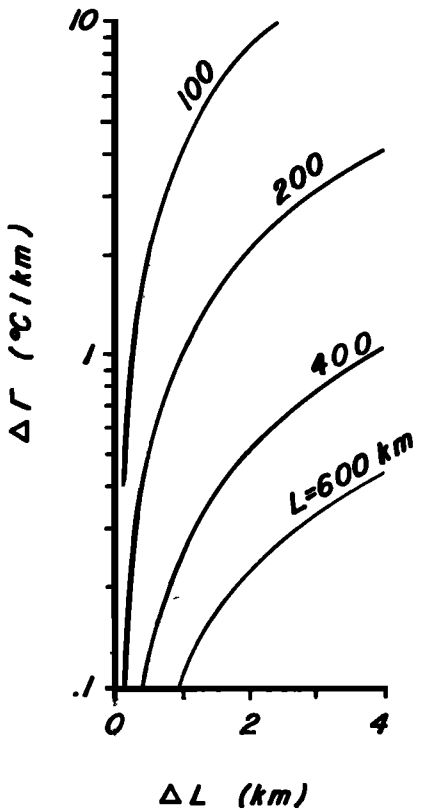

Fig. 13. Compensated thermal expansion ΔL as function of temperature gradient increase $\Delta\Gamma$ for several slab thickness L predicted by the models presented.

for MR than for WO when topography is computed to 400-km depth. The increased temperature gradient at the ridge axis boundary results in newly intruded oceanic material having a temperature excess. This temperature excess in turn gives rise to additional isostatically compensated thermal expansion which accounts for the depth anomaly. Since cooling of oceanic material as it moves away from the ridge axis takes place predominantly in the vertical direction, an element of mass will retain its temperature excess above the temperature of normal ocean as spreading continues (i.e., each follows the same family of cooling curves). Thus the depth anomaly will persist as long as the gradient difference at the axis is maintained. Should this difference cease, subsidence of the ridge axis would precede eventual subsidence of the rest of the ocean to normal depths. Since an increase in the gradient of 0.2°C/km is equivalent to 0.59 mW/m^2 (0.014 HFU) for a conductivity of 2.9 W/m°C (7 mcal/°C cm s), there is no discernible heat flow anomaly.

The response of elevation to a gradient change of only 0.2°C/km was computed for a full 400-km-thick slab. A thinner slab would require a greater gradient increase to produce the same elevation. The interrelation of slab thickness L, gradient increases $\Delta\Gamma$, and the amount of sea floor shallowing ΔL is shown in Figure 13. Any point along a given curve specifies the gradient increase which produces a given depth anomaly. It can be seen that for L = 120 km and shallower the gradient increase is large enough that even for ΔL = 0.1 km a discernible surface heat flow anomaly may be produced. In the Norwegian-Greenland Sea (ΔL = 1 km), a compensation depth of 200 km requires a 1°C/km gradient increase to that depth. In turn, to raise Iceland above sea level, a 'mantle plume' giving rise to a temperature excess down to 200 km would have to increase the gradient by an additional 3°C/km. In other words, the plume must provide an additional heat flow of 8.8 mW/m^2 (0.21 HFU) for a thermal conductivity of 2.9 W/m°C (7 mcal/°C cm s). A very detailed and accurate regional heat flow survey would be required to resolve such an anomaly at the surface. Even if all the compensation for Iceland is placed within the upper 100 km, a 10% or 20% increase in ocean ridge heat flow could produce the excess elevation according to Figure 13. The numbers involved in each of these examples are relatively small and do not appear to rule out the possibility of this mechanism.

If excess thermal expansion down to some depth of compensation is called upon to explain the depth anomaly in the Norwegian-Greenland Sea, then the corresponding density field should produce gravity anomalies which are consistent with the observational data. *Cochran and Talwani* [1978] have compiled the existing gravity and bathymetric data in the North Atlantic including the Norwegian-Greenland Sea. On the basis of 5° × 5° averages, they found that a positive regional depth anomaly of roughly 1 km extending northward into the Norwegian-Greenland Sea from about 30°N coincides with consistently positive free air gravity. A residual free air gravity anomaly of about 20 mgals seems to correlate with the depth anomaly. Computer anlaysis lead *Cochran and Talwani* [1978] to further conclude that at least part of the compensation for excess elevation in the Norwegian-Greenland Sea extends to depths of the order of 300 km. These results can be used to test the thermal depth anomaly model. The density distribution computed from the thermal model has been entered into a computer program [*Takin,* 1967] to compute the gravity anomaly due to excess topography and its compensation for a spherical cap the size of the Norwegian-Greenland Sea. The results are shown in Figure 14 for L = 400 km. The amplitude of the computed gravity anomaly over the center of the topographic anomaly is consistent with the observations. Values for L of less than about 300 km will not produce large enough gravity anomalies to compare with the observed, because compensation of the depth anomaly is too shallow. (It should be pointed out that the *Cochran and Talwani* [1978] compilation is based on shipboard gravity data. Strictly speaking, a more rigorous treatment of the above would incorporate a correction to the geoid.) In the above sense, L, which is obtained from thermal modeling independent of the gravity, may be considered the 'thermal compensation depth.' In the Norwegian-Greenland Sea, it seems

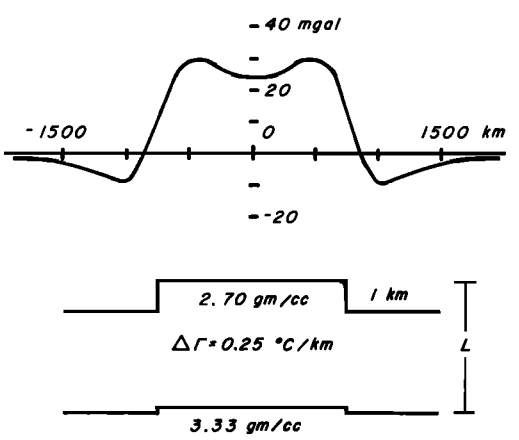

Fig. 14. Gravity anomaly computed for a 1-km thermal depth anomaly.

to coincide with the compensation depth derived from gravity analysis.

DISCUSSION AND SPECULATION

Thermal expansion mechanisms may be capable of reproducing topographic features other than ocean floor subsidence. Such a mechanism was used to simulate the depth anomaly in the Norwegian-Greenland Sea in agreement with the long-wavelength gravity field in that area. The symptoms of this anomaly seem to appear in other broad regions of the world oceans. *Menard* [1973], for example, cites positive depth and gravity anomalies with no apparent heat flow anomaly in the northern Pacific–Gulf of Alaska region. A similar situation seems to exist in the central Pacific for the Hawaiian swell based on compilations of residual gravity and topography [*Watts,* 1976] and regional heat flow [*Sclater and Corry,* 1967; *Sclater et al.,* 1970].

In the model for the Norwegian-Greenland Sea the depth anomaly originated at the ridge axis. This does not necessitate that all large-scale depth anomalies originate at ridge axes. The relationship shown in Figure 13 is equally applicable to a mid-plate thermal anomaly, provided that heat can be brought to the near surface rapidly enough. Often, simple conduction through the lithosphere is too slow to meet this requirement unless large quantities, of heat are introduced from below (*Birch,* 1975). However, in the case of the Hawaiian swell and other mid-plate 'hot spots,' surface volcanism is visual evidence that some heat is being transported to the surface by means other than conduction.

Thermal expansion may also be reflected in shorter-wavelength features. It was shown that much of Iceland's present elevation, for example, could be accounted for by thermal expansion without requiring great amounts of additional heat from below.

That thermal anomalies associated with spreading centers may result from changes or differences in the forces resisting plate motion was first put forth by *Langseth and Zielinski* [1974]. Increased resistance, accordingly, implies more thermal expansion. South of the Southeast Indian Ridge, the ocean floor is significantly shallower than it is to the north [e.g., *Hayes,* 1976]. This could be the result of Antarctica, often assumed fixed in plate motion studies, affording more resistance to sea floor spreading than Australia.

Also suggested is a means by which oceanic material on a continental margin might be elevated above normal ridge crest heights during rifting. (It is conceivable that stresses required to tear plates apart might be greater than those involved in normal sea floor spreading.) Changes in ridge axis elevation with time, from ocean to ocean or along a ridge axis, might also reflect different amounts of resistance to plate motion.

Suppose that sea floor spreading takes place not in a continuous fashion but in a series of rapid surges. Between surges, forces build until the resistive forces are overcome and the plate can move forward. As a result of the motion, energy is dissipated so that driving forces again must build. During the more or less stationary period, material could rise to a greater height at the axis than when the motion is occurring. By adding a periodic component to the ridge axis boundary temperature to simulate this, thermal models could be constructed which reproduce the shorter-wavelength (~10 km) rugged topography common to ridge axes superimposed on the usual ocean floor subsidence curve. Because of lateral cooling, however, this short-wavelength topography would be expected to decay substantially in 10 m.y. (shorter wavelengths decaying more rapidly). So, this mechanism for generating rugged ocean ridge topography suffers from the same problem as the elevated continental margins. That is, while thermal expansion provides a convenient means for generating these features, it does not predict that they will be maintained.

Taken at face value, the changes in temperature gradient required to produce the topographic flucuations mentioned above would imply corresponding fluctuations in magma chemistry. This could provide a test for much of the above speculation. Alternately, it may be more realistic to explore whether or not similar topographic fluctuations might be produced by incorporating a resistive term into the differential equation with a flux boundary condition at the ridge axis instead of the temperature boundary condition which has been used here.

IMPLICATION OF CONVECTION

Apart from the advective term in the conduction equation used here, the model presented ignores heat convection in the earth. This is largely a mathematical convenience. In view of the strong likelihood that in the region beneath the lithosphere (below 100–200 km) convection is the dominant mode of heat transfer, some discussion of the validity of the results presented is warranted.

Thermal models of the lithosphere regardless of whether they are conductive or convective must produce similar temperature fields in the upper 100 km. This is constrained by observations of gravity, topography, surface waves, and geothermometry. Most of the topographic results presented here have been computed from the full 400-km-thick temperature field; however, several cases were discussed in which only the upper 60 km of the region was used to compute topography. All deeper temperature differences were ignored. The effect of varying L for the topographic computation is discussed in more detail in the work of *Zielinski* [1977]. The important result is that, with the exception of the thermal depth anomaly, all features produced by the model remain present as L is reduced to about 100 km. This magnitudes of both the ocean floor subsidence and the topographic edge effect are in fact greater when only the upper 160 km of the temperature field is used for the computation than when the entire 400 km is used. In view of these facts, it seems likely that the topography generated from the temperature field of a purely convective model which simultaneously incorporates ocean and continent would exhibit effects similar to those presented here.

The lower half of the 400-km temperature field contributes little to the topographic effects. This is because the mean lateral heat transfer in this region is considerably less than for the upper 200 km. To this approximation, as was stated earlier, the lateral motion of the lower half of the region is insignificant (i.e., the model is not meant to suggest a 400-km-thick lithosphere). Below 200 km, the model produces vertical temperature gradients which are nearly adiabatic, so the temperature field in the lower region is not greatly different from that produced by some convective models [e.g., *Schubert et al.,* 1978]. For these reasons, the model presented here may be considered an approximation to its more elegant but less tractable convective counterpart.

Acknowledgments. I am grateful for the assistance and comments of my colleagues at Lamont and would particularly like to thank M. G. Langseth and A. B. Watts.

REFERENCES

Birch, F. S., Conductive heat flow anomalies over a hot spot in a moving medium, *J. Geophys. Res., 80,* 4825–4827, 1975.

Bottinga, Y., and C. J. Allegre, Thermal aspects of seafloor spreading and the nature of the oceanic crust, *Tectonophysics, 18,* 1–17, 1973.

Clark, S. P., and A. E. Ringwood, Density distribution and constitution of the mantle, *Rev. Geophys. Space Phys., 2,* 35–88, 1964.

Cochran, J. R., and M. Talwani, Gravity anomalies, regional elevation, and the deep structure of the North Atlantic, *J. Geophys. Res., 83,* 4907–4924, 1978.

Forsyth, D. W., Evolution of the upper mantle beneath mid-ocean ridges, *Tectonophysics, 38,* 89–118, 1977.

Foucher, J. P., and X. Le Pichon, Comments on thermal effects of the formation of Atlantic continental margins by continental break-up by N. H. Sleep, *Geophys. J. Roy. Astron. Soc., 29,* 43–46, 1972.

Froidevaux, C., and G. Schubert, Plate motion and structure of the continental asthenosphere: A realistic model of the upper mantle, *J. Geophys. Res., 80,* 2553–2564, 1975.

Froidevaux, C., G. Schubert, and D. A. Yuen, Thermal and mechanical structure of the upper mantle: A comparison between continental and oceanic models, *Tectonophysics, 37,* 233–246, 1977.

Haenel, R., Heat flow measurements in the Norwegian Sea, *Meteor Forsch-Ergebnisse C, 17,* 74–78, 1974.

Haller, J., *Geology of the East Greenland Caledonides,* Interscience, New York, 1971.

Hayes, D. E., Nature and implications of asymmetric sea-floor spreading—Different rates for different plates, *Geol. Soc. Amer. Bull., 87,* 994–1002, 1976.

Hays, J. D., and W. C. Pitman III, Lithospheric plate motion, sea level changes, and climatic and ecological consequences, *Nature, 246,* 18–22, 1973.

Holtedahl, O., On supposed marginal faults and the oblique uplift of the land mass in Cenozoic time, in *Geology of Norway: Norges Geol. Undersökelser,* no. 208, pp. 351–357, Oslo, 1960.

Johnson, G. L., Morphology of the mid-ocean ridge between Iceland and the Arctic basin, in *Geodynamics of Iceland and the North Atlantic Area,* edited by Kristjansson, pp. 49–62, 1974.

Jordan, T. H., The continental tectosphere, *Rev. Geophys. Space Phys., 13,* 1–12, 1975.

Lachenbruch, A. H., Crustal temperature and heat production: Implications of the linear heat flow relation, *J. Geophys. Res., 75,* 3291–3300, 1970.

Langseth, M. G., Jr., and G. W. Zielinski, Marine heat flow measurements in the Norwegian-Greenland Sea and in the vicinity of Iceland, in *Geodynamics of Iceland and the North Atlantic Area,* edited by Kristjansson, pp. 277–295, 1974.

Langseth, M. G., Jr., X. Le Pichon, and M. Ewing, Crustal structure of the mid-ocean ridges, 5, Heat flow through the Atlantic Ocean floor and convection currents, *J. Geophys. Res., 71,* 5321–5355, 1966.

McKenzie, D. P., Some remarks on heat flow and gravity anomalies, *J. Geophys. Res., 72,* 6261–6273, 1967.

McKenzie, D. P., Some remarks on the development of sedimentary basins, *Earth Planet. Sci. Lett., 40,* 25–32, 1978.

Menard, H. W., Depth anomalies and the bobbing motion of drifting islands, *J. Geophys. Res., 78,* 5128–5137, 1973.

Minister, J. B., and C. B. Archambeau, Systematic inversion of continental heat-flow and temperature data (abstract), *Eos Trans. AGU, 51,* 824, 1970.

Parsons, B., and J. G. Sclater, An analysis of the variation of ocean floor heat flow and bathymetry with age, *J. Geophys. Res., 82,* 803–827, 1977.

Schatz, J. F., and G. Simmons, Thermal conductivity of earth materials at high temperatures, *J. Geophys. Res., 77,* 6966–6983, 1972.

Schubert, G., D. A. Yuen, C. Froidevaux, L. Fleitout, and M. Souriau, Mantle circulation with partial shallow return flow: Effects of stresses in oceanic plates and topography of the sea floor, *J. Geophys. Res., 83,* 745–758, 1978.

Sclater, J. G., and C. E. Corry, Heat flow, Hawaiian area, *J. Geophys. Res., 72,* 3711–3715, 1967.

Sclater, J. G., and J. Francheteau, The implications of terrestrial heat-flow observations on current tectonic and geochemical models of the crust and upper mantle of the earth, *Geophys. J. Roy. Astron. Soc., 20,* 509–542, 1970.

Sclater, J. G., J. D. Mudie, and C. G. A. Harrison, Detailed geophysical studies on the Hawaiian Arch near 24°25'N, 157°40'W: A closely spaced suite of heat flow stations, *J. Geophys. Res., 75,* 333–348, 1970.

Sclater, J. G., R. N. Anderson, and M. LeeBell, Elevation of ridges and evolution of the central eastern Pacific, *J. Geophys. Res., 76,* 1888–1915, 1971.

Sclater, J. G., J. Crowe, and R. N. Anderson, On the reliability of oceanic heat flow averages, *J. Geophys. Res., 81,* 2997–3006, 1976.

Sleep, N. H., Thermal effects of the formation of Atlantic continental margins by continental break-up, *Geophys. J. Roy. Astron. Soc., 24,* 325–350, 1971.

Swanberg, C. A., G. Simmons, M. D. Chessman, G. Grønlie, and K. S. Heier, Heat flow heat generation studies in Norway, *Eos Trans. AGU, 54,* 464, 1973.

Takin, M., Interpretation of gravity anomalies using computers, Ph.D. thesis, Pembroke Coll., Cambridge, Mass., 1967.

Talwani, M., and O. Eldholm, Continental margin off Norway: A geophysical study, *Geol. Soc. Amer. Bull., 83,* 3575–3606, 1972.

Talwani, M., and O. Eldholm, Evolution of the Norwegian-Greenland Sea, *Geol. Soc. Amer. Bull., 88,* 969–999, 1977.

Wager, L. R., Geological investigations in East Greenland, IV, The stratigraphy and tectonics of Knud Rasmussents Land and the Kangerlagssuaq Land and the Kangerlagssuaq region, *Medd. Groenland, 134,* 1–64, 1947.

Walcott, R., Gravity, flexure, and growth of sedimentary basins at a continental edge, *Geol. Soc. Amer. Bull., 83,* 1845–1848, 1972.

Watts, A. B., Gravity and bathymetry in the Central Pacific Ocean, *J. Geophys. Res., 81,* 1533–1553, 1976.

Watts, A. B., and W. B. F. Ryan, Flexure of the lithosphere and continental margin basins, *Tectonophysics, 36,* 25–44, 1976.

Zielinski, G. W., Thermal history of the Norwegian-Greenland Sea and its rifted continental margin, Ph.D. thesis, Columbia Univ., New York, 1977.

(Received August 15, 1978;
revised June 20, 1979;
accepted June 29, 1979.)